iScience

CellPress
OPEN ACCESS

Article

Neuronal reprogramming of mouse and human fibroblasts using transcription factors involved in suprachiasmatic nucleus development

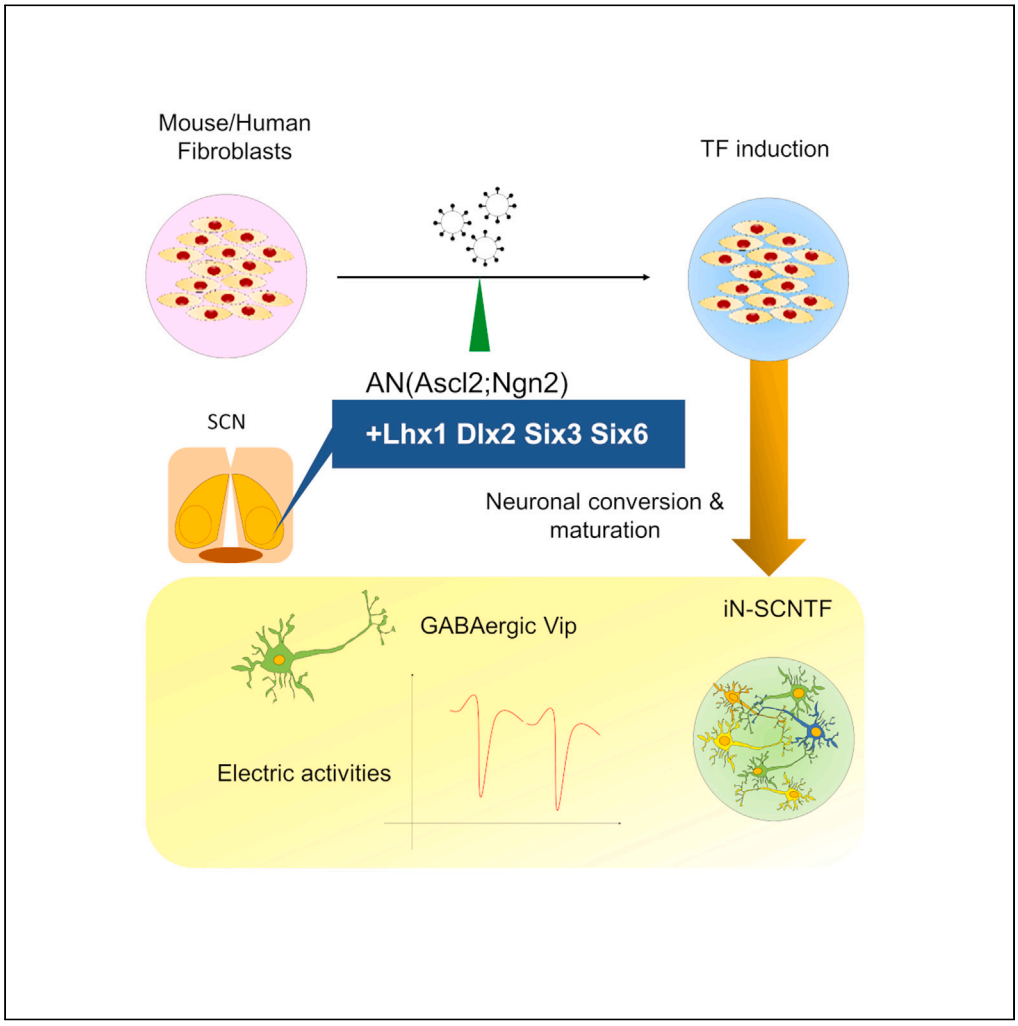

Masatoshi Hirayama, Ludovic S. Mure, Hiep D. Le, Satchidananda Panda

panda@salk.edu

Highlights

Induced neurons were generated with SCN-related transcription factors (iN-SCNTF)

The iN-SCNTF was GABAergic, vasoactive intestinal peptide (Vip) positive neurons

The iN-SCNTF were capable of exhibiting robust circadian rhythms in neuron firing

The iN-SCNTF may represent Vip-expressing neuronal subtypes in the SCN

Hirayama et al., iScience 27, 109051
March 15, 2024
https://doi.org/10.1016/j.isci.2024.109051

iScience

CellPress
OPEN ACCESS

Article

Neuronal reprogramming of mouse and human fibroblasts using transcription factors involved in suprachiasmatic nucleus development

Masatoshi Hirayama,[1,2] Ludovic S. Mure,[1,3,4] Hiep D. Le,[1] and Satchidananda Panda[1,5,*]

SUMMARY

The hypothalamic suprachiasmatic nucleus (SCN) is composed of heterogenous populations of neurons that express signaling peptides such as vasoactive intestinal polypeptide (VIP) and arginine vasopressin (AVP) and regulate circadian rhythms in behavior and physiology. SCN neurons acquire functional and morphological specializations from waves of transcription factors (TFs) that are expressed during neurogenesis. However, the *in vitro* generation of SCN neurons has never been achieved. Here we supplemented a highly efficient neuronal conversion protocol with TFs that are expressed during SCN neurogenesis, namely *Six3*, *Six6*, *Dlx2*, and *Lhx1*. Neurons induced from mouse and human fibroblasts predominantly exhibited neuronal properties such as bipolar or multipolar morphologies, GABAergic neurons with expression of VIP. Our study reveals a critical contribution of these TFs to the development of vasoactive intestinal peptide (Vip) expressing neurons in the SCN, suggesting the regenerative potential of neuronal subtypes contained in the SCN for future SCN regeneration and *in vitro* disease remodeling.

INTRODUCTION

The suprachiasmatic nucleus (SCN) resides in the hypothalamus and regulates daily circadian rhythms in physiology and behavior.[1,2] The SCN consists of a heterogeneous population of ~20,000 neurons, which exhibit cell-autonomous intrinsic rhythms in electrical activity. These rhythms are generated at the molecular level by interacting feedback loops involving the transcription and translation of clock genes.[1] Neurotransmitters and neuropeptides play important roles in inter-cellular communication between SCN neurons. This communication synchronizes period length and phase among SCN neurons resulting in uniform and robust circadian oscillations.[3,4] One feature of the SCN network that is conserved across vertebrate species is the non-overlapping expression of the neurotransmitters vasoactive intestinal polypeptide (VIP) and arginine vasopressin (AVP), which are expressed in the core and shell regions of the SCN, respectively.[3,5] In addition, nearly all SCN neurons express γ-aminobutyric acid (GABA).[6,7] SCN neuronal network coupling via neurotransmitters such as VIP and GABA is critical for the oscillation, phase-shift, and synchronization of SCN neurons *in vitro* and *in vivo*.[8,9] AVP can also restore synchronous rhythms in SCN neurons that lack VIP,[10,11] suggesting that VIP, GABA, and AVP are important to maintain intercellular synchrony within the SCN.[8,9,12]

The development of SCN neurons is well understood. During embryonic hypothalamic development, the SCN develops from the neuroepithelium caudal to the optic recess.[13] After birth, the SCN continues to mature, beginning to express major neuropeptides and receiving input from retinal nerve fibers. Previous studies have characterized spatial and temporal patterns of gene expression in the SCN, revealing that specific transcription factors (TFs) are expressed in subsets of SCN neurons during pre-and post-natal development.[14] First, regional changes in neurogenesis within the embryonic SCN region are associated with the expression of TFs like *Six3*, *Six6*, *Fzd5*, and a transient increase in (retinal homeobox protein Rx) *Rx* expression. Transient expression of TF Rx has a possibility to contribute to regulation of SCN location and cell number by an unknown mechanism.[14] Early post-mitotic SCN neurons are characterized by the expression of *Six3*, *Six6*, *Lhx1*, and *Dlx2*, followed by expression of the neuropeptides VIP and AVP.[14] While these core TFs contribute to the specification and maturation of SCN neurons, as well as to circadian function,[14–17] it is unknown whether these core TFs contribute to neurogenesis in the SCN.

TF-based cell reprogramming, in which somatic cells are converted into pluripotent or alternative somatic cell fates, has revealed that cell differentiation is not a unidirectional phenomenon.[18–20] Several laboratories have demonstrated that pan-neurons can be generated by overexpressing neuronal TFs. Researchers are now focused on identifying combinations of TFs that can induce specific neuronal subtypes. Understanding diseased neurons derived from patient-derived iPS cells may lead to therapeutic approaches.[21]

[1]Regulatory Biology Laboratory, Salk Institute for Biological Studies, La Jolla, CA, USA
[2]Department of Ophthalmology, School of Medicine, Keio University, Tokyo, Japan
[3]Department of Ophthalmology, Inselspital, Bern University Hospital, University of Bern, Bern, Switzerland
[4]Department of BioMedical Research, University of Bern, Bern, Switzerland
[5]Lead contact
*Correspondence: panda@salk.edu
https://doi.org/10.1016/j.isci.2024.109051

Chronic disruption of circadian rhythms is associated with a wide variety of pathological processes, including aging, cancer, metabolic, neuropsychiatric, and neurodegenerative disorders.[22–25] However, there is still no *in vitro* model for studying the SCN aging or degeneration. Previous study on allogenic fetal SCN transplants and SCN-lesioned hosts showed that the SCN is the dominant circadian pacemaker and suggested the concept of reconstruction of circadian clock disorders by SCN transplantation.[26,27] A few studies in rodents have reported the graft showed extensive fiber outgrowth from the implant into the host hypothalamus, functional replacement of the SCN by transplanting allogenic SCN grafts derived from embryonic tissue, restoring several aspects of circadian behavioral rhythms.[26,28–30] Hence, using *in vitro* reprogramming to generate neurons of the SCN would represent a critical tool for studying mechanisms of SCN development and disease-associated pathologies, as well as for generating cells for regenerative medicine approaches.

In this study, we directly converted mouse and human fibroblasts into neurons with Vip-expressing neuronal phenotypes in the SCN, thereby generating induced SCN neurons (iN-SCNTFs). These analyses reveal that subpopulations of SCN neurons can be differentiated from human cells. The advancement about the contribution of TFs to the differentiation of Vip-expressing neurons suggest feasibility of regeneration of specific SCN neuronal subtypes via direct reprogramming, which is an important step in the process of realizing SCN regenerative medicine and *in vitro* models. This advancement will pave the way toward establishing *in vitro* models of diseases associated with circadian disruption and enable the development of regenerative medicine approaches for treating affected patients.

RESULTS

Efficient conversion of mouse embryonic fibroblasts into neurons

A series of influential studies have demonstrated that functional neurons can be generated from both stem and somatic cell types via direct cell conversion.[31] Human fibroblasts can be efficiently converted into neurons using the pro-neuronal TFs *Ascl1* (*Mash1*) and *Ngn2* together with small molecule inhibitors of glycogen synthase kinase 3β and SMAD signaling.[32] To build upon these results, we first investigated whether we could use this neural conversion method to generate induced neurons (iNs) from mouse embryonic fibroblasts (MEFs) (Figure 1A). We confirmed that MEFs do not express the neural progenitor maker, Sox2, the neuronal markers, βIII-tublin (βIII-tub) and Map2ab, or the neural crest progenitor antigen, p75. We then transduced MEFs with a mixture of doxycycline (dox)-inducible lentivirus that express *Ascl1* and *Ngn2* (AN) (Figures S1A–S1C). Treatment with doxycycline resulted in efficient and robust transgene expression; no AN expression was detected in doxycycline-free conditions (Figure S2).[33] Cells were grown in a neuronal conversion culture environment along with small molecule inhibitors, and four weeks later the cultures contained βIII-tub$^+$ cells with neuron-like morphology.[33] To characterize the dynamics of this conversion process we performed a time-series analysis. We found βIII-tub immunostaining at days 7, 14, 21, and 28. The percentage of βIII-tub$^+$ cells in these cultures was approximately 50% at day 7 and all subsequent time points (Figures 1B, 1C, S1D, and S1E). By contrast, βIII-tub$^+$ cells were not observed when cells were cultured without the neuronal conversion culture environment. We further found that these iNs also expressed Map2ab, a marker of mature neurons, and developed dendritic structures by day 28 (Figures 1B and 1D). These results suggest that the AN/small-molecule strategy enables highly efficient conversion of MEFs to iNs that express a number of neuronal markers.

While previous studies have generated heterogeneous populations of iNs, it remains unclear whether specific SCN neuronal subtypes can be induced.[32] In an attempt to generate iNs with SCN-related TFs (iN-SCNTF) we modified the AN/small-molecule neuronal conversion process by adding lineage-specific TFs that act during SCN development.[34,35] We searched published literature to find TFs expressed in an SCN-specific manner and essential for SCN function. As we have reported previously,[17] we had identified 13 TFs (Dlx2, Dlx6, Foxd1, Gatad2b, Hsf2, Lhx1, Nr2f2, Rorα, Rorβ, Six3, Sox1, Sox11, and Tle4) from comparing the transcriptome data of the SCN with that of 82 other mouse tissues including 14 different neural tissues to identify SCN enriched TFs[36](Table S1). We have also found that Lhx1 is critical for SCN neurons to generate circadian rhythms.[17] Furthermore, the developmental gene expression analysis of the SCN from VanDunk et al.[14] showed six TFs (of which four were the same as our candidate TFs), which were confirmed to be expressed during SCN development periods with the post-mitotic cells. As a result, 15 TFs became candidates (Table S1). We selected four TFs from our list for the current study because they were confirmed to be expressed in post-mitotic SCN cells (Lhx1, Dlx2, Six3, and Six6).[14,17,37] Mice carrying loss-of-function alleles for some of these TFs show severe deficits in SCN differentiation or SCN-specific expression of neuropeptides.[14,38–40] MEFs were transduced with a mixture of doxycycline (dox)-inducible lentiviruses expressing *Lhx1*, *Dlx2*, *Six3*, *Six6*, and AN (Figure S1). Immunostaining analysis revealed that the percentage of βIII-tub$^+$ cells was approximately 50% on both day 7 and day 28 (50.4 ± 4.0% and 44.4 ± 9.7%, respectively). This was consistent with our iN results (Figures 1B and 1C). At day 28, the majority of iN-SCNTFs also expressed Map2ab (Figures 1B and 1D). These results indicate that our modified neuronal conversion strategy induced cells that express neuronal markers at efficiencies similar to iN protocols.

Previous reports have revealed that neurons within the SCN have specific neuronal characteristics. For example, NeuN is another marker of mature neurons (recently identified as Fox3), but in the SCN it does not co-localize with VIP- or AVP-immunoreactive neurons.[5] Therefore, we asked whether iNs and iN-SCNTFs express NeuN by immunostaining. We found that NeuN was expressed by fewer βIII-tub$^+$ iN-SCNTFs than iNs (2.5 ± 0.4% of iN-SCNTF neurons, 33.3 ± 5.9% of iNs) (Figures 1E and 1F). This is one feature of iN-SCNTFs that is distinct from iNs. Next, we further investigated the neuronal properties of iN-SCNTFs.

Reprogrammed cells exhibit characteristics of SCN neurons

Almost all SCN neurons release the neurotransmitter GABA, which is the major inhibitory neurotransmitter in the brain, and express GABA receptors. Morphologically, many SCN neurons are bipolar or multipolar (two or more dendrites, respectively).[41,42] Further, GABAergic signaling is critical for phase shifting in the SCN.[43] Thus, we conducted immunohistochemical analyses to compare neurotransmitter

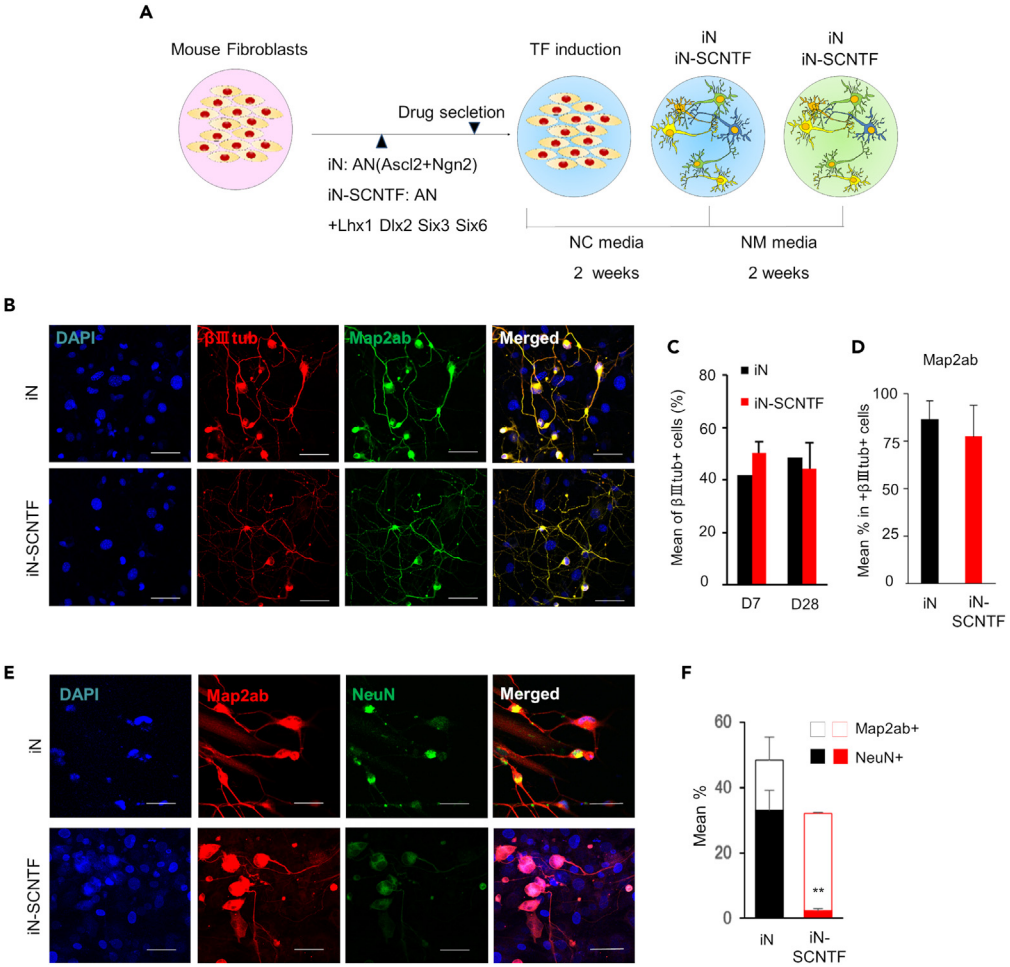

Figure 1. Overexpression of SCN developmental transcription factors for neuronal trans-differentiation of mouse fibroblasts

(A) Schematic image shows the *trans*-differentiation strategy and timeline for inducing mouse fibroblasts to neurons using two neuronal transcription factors (AN: ASCL1 and NGN2) and to iN-SCNTF neurons with four additional transcription factors (LHX1, DLX2, SIX3, and SIX6).

(B) Immunofluorescence analysis of iN (upper panels) and iN-SCNTF (lower panels) 4 weeks post conversion shows efficient conversion of βIII-tublin expression (red) and Map2ab. expression (green). DAPI counterstained nuclei (blue); quantification shown in (C) and (D). No significant difference in βIII-tublin positive cell rate between iN and iN-SCNTF (D7, $p = 0.1580$, D28 $p = 0.6742$, Student's t test). No significant difference in Map2ab cell rate between iN and iN-SCNTF ($p = 0.5099$, Student's t test). Scale bars: 50μm.

(E) Immunofluorescence images show Map2ab expression (red) and NeuN expression (green) in iN (upper panels) and iN-SCNTF (lower panels) 4 weeks post conversion. DAPI counterstained nuclei (blue); quantification shown in (F). (**$p < 0.001$, Chi-squared test) Scale bars: 50μm.

properties of iN-SCNTFs and iNs. For iNs, 18.1 ± 5% of βIII-tub$^+$ neurons were immunopositive for the GABA synthetic enzymes GAD65/67 and 63.4 ± 4% expressed VGlut1, a vesicular glutamate transporter characteristic of glutamatergic neurons. For iN-SCNTFs, 83.9 ± 6% of βIII-tub$^+$ cells were GABAergic (GAD65/67$^+$) and 15.8 ± 5% were glutamatergic. Thus, as seen in the SCN, iN-SCNTFs were mostly GABAergic (Figures 2A–2C). We assessed the morphology of reprogrammed neurons and found that the majority of iN-SCNTFs were bipolar or multipolar, whereas iNs were predominantly monopolar (one primary dendrite) (Figure 2D). These results suggest that iN-SCNTFs are more similar to SCN neurons than to iNs.

Expression of neuropeptides mediating circadian rhythmic oscillation

We hypothesized that the TFs we used to generate iN-SCNTFs are crucial for the differentiation and function of two principal subpopulations of SCN neurons, namely GABAergic neurons that express the neuropeptides VIP and AVP. Thus, we prepared Vip-Cre; R26-CAG-LSL-Sun1-sfGFP-myc (Vip^{cre};Sun1^{sfGFP}) mice and Avp-Cre; R26-CAG-LSL-Sun1-sfGFP-myc (Avp^{cre};Sun1^{sfGFP}) mice to label cells expressing these neuropeptides. Because retinoic acid-related orphan receptor alpha (Rorα), which is important for the clock function in post-mitotic neurons in the entire or peripheral SCN, we also generated Rorα^{cre};Sun1^{sfGFP} mice. Rorα expression does not affect SCN development or function. In each of these mice, the SUN1 fusion protein (SUN1 fused to sfGFP) localizes to the inner nuclear membrane of cell types expressing

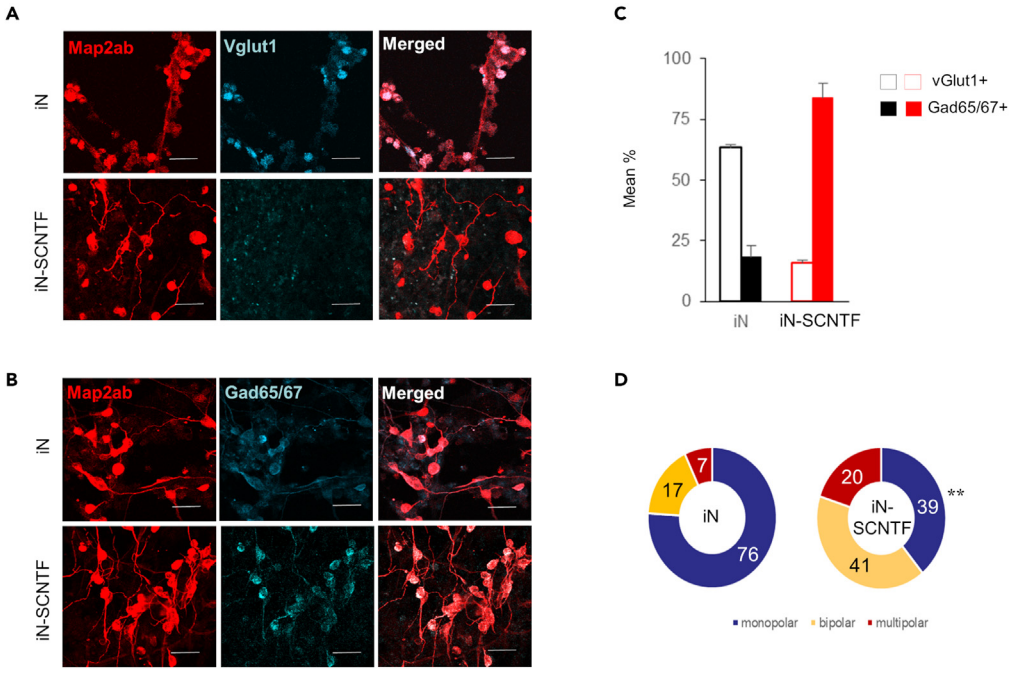

Figure 2. The characteristic neuronal properties in the differentiated neurons

(A) Immunofluorescence analysis shows expression of glutamatergic neuronal markers, VGlut1 (a glutamate transporter, blue) in iN (upper panels) and iN-SCNTF (lower panels) 4 weeks post conversion. Map2ab; red. Scale bars: 50μm.

(B) Immunofluorescence analysis shows expression of GABAergic neuronal markers, GAD65/67 (glutamate decarboxylase, blue) in iN (upper panels) and iN-SCNTF (lower panels) 4 weeks post conversion. Map2ab; red. Quantification shown in (C). Scale bars: 50μm.

(D) Morphological analysis of neuronal properties of iN and iN-SCNTF (monopolar vs. bi-/multipolar **$p < 0.001$ Chi-squared test).

Cre recombinase[44] (Figure S4). We confirmed correct GFP localization in the brains of Vip^{cre};Sun1^{sfGFP} mice (the ventrolateral "core" region of the SCN), Avp^{cre};Sun1^{sfGFP} mice (the dorsomedial "shell" region of the SCN) and the paraventricular nucleus (PVN) and Rorα^{cre};Sun1^{sfGFP} mice (the entire SCN) (Figure S4). We found that GFP-positive cells in Vip^{cre};Sun1^{sfGFP} and Avp^{cre};Sun1^{sfGFP} mice expressed VIP and AVP, respectively (Figure 3A). These data suggest that GFP reflects target gene expression in these mice.

We next investigated whether our neuronal conversion method could generate neurons that express neuropeptides important for circadian oscillation in the SCN. We generated iNs and iN-SCNTFs from MEF isolated from these transgenic mice and analyzed patterns of GFP. In cells induced from Vip^{cre};Sun1^{sfGFP} mice, 11.4 ± 1.5% of βIII-tub$^+$ iN-SCNTFs were GFP-positive, whereas <1% of βIII-tub$^+$ iNs were Gfp$^+$. For βIII-tub$^+$ cells generated from Avp^{cre};Sun1^{sfGFP} mice, 2.1 ± 1.4% of iN-SCNTFs and 1.6 ± 1.2% of iN were GFP$^+$. Finally, for Rorα^{cre};Sun1^{sfGFP} mice, 2.8 ± 0.8% of βIII-tub$^+$ iN-SCNTFs and 0.5% ± 0.4% of βIII-tub$^+$ iNs were GFP$^+$ (Figures 3B and 3C). There was significant difference in GFP positive neurons derived from Vip^{cre};Sun1^{sfGFP} mice and Rorα^{cre};Sun1^{sfGFP} mice between iN and iN-SCNTF (Vip; $p = 0.0052$, Rorα; $p = 0.0197$, Avp; $p = 0.3831$, Student's t test). Quantitative mRNA expression analysis also revealed that the expression of Vip, Avp, Grp (another SCN neuronal peptide) was increased in iN-SCNTF compared to iN, and that Rorα also tended to be increased (Figure S5). These results indicated that iN-SCNTFs include neurons that express SCN-related genes like Avp and *Rorα*, as well as those that express VIP. Based on the aforementioned results, we hypothesized that our TF cocktail is mainly involved in the development of Vip-expressing neurons in the SCN neuronal population, and we therefore further characterized the neuronal characteristics of Vip-expressing iN-SCNTFs, which were the largest subpopulation of iN-SCNTF culture. VIP-expressing GABAergic neurons in the core of the SCN play a critical role in generating the circadian cycle and synchrony among SCN neurons.[45] After an extended culture period to generate fully mature iN-SCNTFs from Vip^{cre};Sun1^{sfGFP} MEFs, we confirmed that GFP$^+$ neurons expressed VIP (Figure 3D). In addition, these VIP expressing neuron was observed with co-expression of GAD67 in iN-SCNTF culture. Via immunostaining, we further confirmed the co-expression of VIP and GAD67 in these iN-SCNTFs (Figure 3E). These results indicate that iN-SCNTFs contain VIP-expressing iN-SCNTFs GABAergic neurons.

Generation of iN-SCNTFs from human fibroblasts

Fibroblasts are relatively easy to obtain from human patients, and it is thought that differentiation of these cells into specific neuronal subtypes will be a transformative step toward developing *in vitro* models of neurological disease and new regenerative therapies (e.g., cell transplantation and pharmacological interventions).[46,47] Therefore, we asked whether we could generate iN-SCNTFs from human fibroblasts using our TF-based differentiation protocol. After extended culturing (6 weeks) of human skin-derived fibroblasts in the maturation environment with

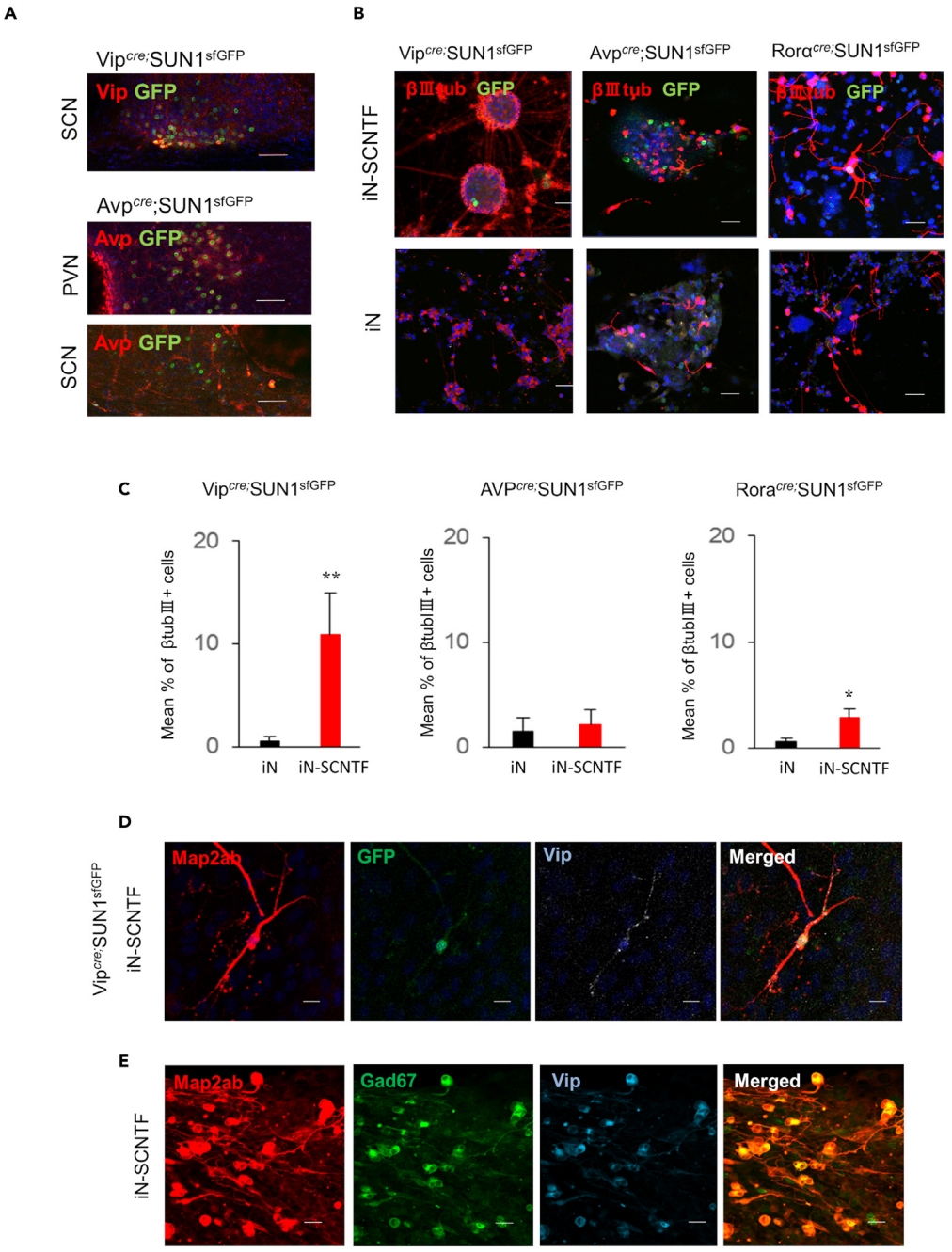

Figure 3. Neuronal conversion using mouse fibroblasts from transgenic mice such as Vip^{cre};Sun1^{sfGFP} mice, Avp^{cre};Sun1^{sfGFP} mice and Rorα^{cre};Sun1^{sfGFP} mice

(A) Immunofluorescence histological analysis of SCN or PVN tissues of transgenic mice. Vip; red, GFP; green. Scale bars: 100μm.

(B) Immunofluorescence analysis shows expression of GFP in iN (lower panels) and iN-SCNTF (upper panels) from transgenic mouse fibroblasts 4 weeks post conversion. βIII-tublin; red. Quantification shown in (C). (Vip; **p = 0.0052, Rorα; *p = 0.0197, Avp; p = 0.3831, Student's t test) Scale bars: 50μm.

(D) Representative Immunofluorescence images of Vip-expressing iN-SCNTF neurons derived from Vip^{cre};Sun1^{sfGFP} mouse fibroblasts. Scale bars: 50μm.

(E) Representative Immunofluorescence images of Vip (blue) and Gad67 (green) expression in iN-SCNTF. Scale bars: 50μm.

mouse astrocyte feeder cells, we assessed the extent of neuronal differentiation (Figure 4A). After confirming that all βIII-tub$^+$ cells in the iN and iN-SCNTF cultures were derived from human fibroblasts, we analyzed the neuronal conversion rate (Figures 4B and 4C). Fibroblasts subjected to iN or iN-SCNTF protocols differentiated into βIII-tub$^+$ cells at the rate of 75.9 ± 4.2% and 37.2 ± 2.4%, respectively. As we observed for iN-SCNTFs derived from MEFs, fewer iN-SCNTFs expressed NeuN (2.5 ± 1.9%) than seen in iN cultures (40.6 ± 13.1%). More iN-SCNTFs

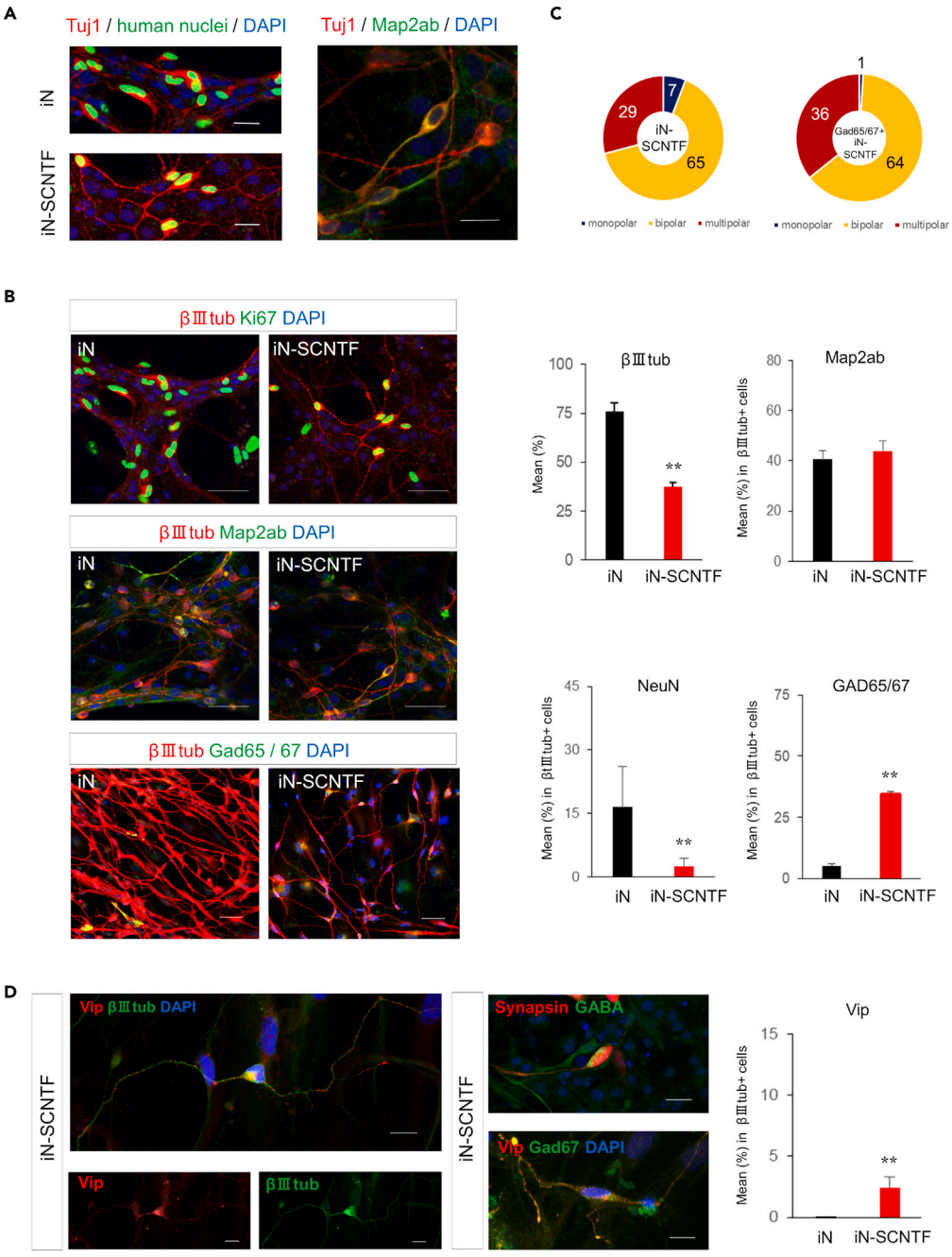

Figure 4. Neuronal conversion using mouse fibroblasts from human fibroblasts

(A) Immunofluorescence images show βIII-tublin expression (red) and Ki67, human nuclei marker, expression (green) in iN (upper panels) and iN-SCNTF (lower panels) 4 weeks post conversion. DAPI counterstained nuclei (blue); Scale bars: 25μm.

(B) Immunofluorescence analysis of iN (upper panels) and iN-SCNTF (lower panels) 4 weeks post conversion shows efficient conversion of βIII-tublin expression (red) and Map2ab expression (green). Lower rate in neuronal conversion with βIII-tublin expression was observed (βIII-tublin; **$p < 0.001$ Student's t test, Map2ab; $p = 0.4188$ Student's t test) NeuN positive rate was significantly lower in iN-SCNTF, and GAD65/67 rate was significantly higher in iN-SCNTF (NeuN **$p = 0.0084$ Student's t test, GAD65/67 **$p < 0.001$ Student's t test) DAPI counterstained nuclei (blue). Scale bars: 20 μm.

(C) Proportion (in %) of neurons that were uni-, bi- or multi-polar.

(D) Morphological analysis of neuronal properties of human iN and iN-SCNTF. Vip positive rate was significantly higher in iN-SCNTF than in iN (**$p = 0.0084$ Student's t test).

from human fibroblasts were GABAergic than seen for iNs (34.2% ± 1.3% of iN-SCNTFs, 5.0 ± 1.0% of iNs). There was also a small population of VIP-expressing GABAergic iN-SCNTFs (Figure 4D). Morphologically, these iN-SCNTFs were mostly bi- and multi-polar. These results indicated that it may be possible to generate iN-SCNTFs with SCN neuronal subtype phenotypes from human fibroblasts.

Electrophysiological activity to generate circadian rhythm in iN-SCNTFs

To functionally assess our iN-SCNTFs we analyzed their electrophysiological properties. These included spontaneous action potentials and circadian changes in the rate of action potential firing (Figure 5). Six-week-old induced cell cultures maintained on primary rat astrocytes or dispersed mouse primary SCN neurons (pSCNs) were loaded with the calcium-sensitive dye Fluo-4. We then recorded neuronal activity with time-lapse imaging for approximately 3 min iN-SCNTFs exhibited spontaneous calcium transients, suggesting that they were spontaneously active (Figure 5A). In addition, we found that there was a significant difference in the maximum ΔF/F between iN and iN-SCNTF ($p < 0.001$, Student's t test), or iN and pSCN ($p < 0.001$, Student's t test), but there was no significant difference between iN-SCNTF and pSCN ($p = 0.0697$, Student's t test). We also found that there was a significant difference in the number of spikes in 3 min (spike rhythm) between iN and iN-SCNTF ($p = 0.0114$, Student's t test), or iN and pSCN ($p = 0.0030$, Student's t test), but there was no significant differences between iN-SCNTF and pSCN ($p = 0.4169$, Student's t test). These results indicated that some iN-SCNTFs exhibited calcium transients that were higher in amplitude and lower in frequency than seen with iNs. Such iN-SCNTF calcium transients were similar to those seen in pSCN (Figures 5B and 5C).

Neurons in the SCN exhibit endogenous circadian rhythms in electrical activity. To record cellular rhythms of individual cells, we cultured iN-SCNTFS, iNs, and pSCNs on multi-microelectrode arrays (MEAs) (Figures 5D, 5E, 5F, and S6) and monitored circadian patterns of spontaneous firing for 2–3 days. Both pSCNs and iN-SCNTFs showed robust rhythms and free-run independent of each other, as reported previously for the rodent SCN.[42,48] No specific firing patterns were observed in iN cultures. iN-SCNTFs in the same MEA culture plate exhibited a range of circadian periods and phase relationships, suggesting that iN-SCNTFs are capable of exhibiting robust circadian rhythms in neuron firing.

DISCUSSION

There is a long history of attempts to establish SCN neurons *in vitro* to study their molecular and cellular properties. Oncogene-induced immortalization of embryonic SCN neurons from rodents has been used to generate SCN cell lines that can be propagated and studied.[49] Previous reports suggested circadian rhythmicity can be restored by transplantation of fetal anterior hypothalamic tissue containing the SCN into hosts rendered arrhythmic by SCN ablation.[28,29,50] The transplanted SCN-derived VIP neuronal fibers were integrated with the host brain and could be identified in host terminal fields typically innervated by SCN-VIP fibers.[51] While it was reported that circadian neuroendocrine rhythms are not reestablished by the SCN grafts,[30] SCN grafts could restore rhythmicity in the PVN of the hypothalamus.[52] For the restoration of rhythmicity, it requires that the grafts contain a minimum volume of SCN tissues with cytoarchitecture including VIP and AVP neurons, and VIP-expressing neurons are critical component to functional recovery.[53] Success in using such SCN cell lines to restore circadian activity rhythms in SCN-ablated (and consequently arrhythmic) rats has demonstrated the promise of implanting SCN neurons to restore circadian rhythms of activity and rest in patients with neurodegenerative diseases such as Alzheimer's disease.[26] To date, however, SCN cell lines have been generated using embryonic SCN cells as starting material. Thus, this approach has inherent limitations for studying the mechanisms of circadian disorders.

In this study we leveraged advancements in two fields of study: (1) understanding SCN ontogeny, and (2) the direct reprogramming of neuronal subtypes from various cell types, including MEFs. Generating iNs using the Ascl1/Ngn2 protocol yielded many glutamatergic neurons, a smaller number of GABAergic neurons, and single dopaminergic and serotonergic neurons.[33] Although this ensemble of neuronal subtypes is very different from the SCN, iN conversion is highly plastic and researchers have successfully induced the differentiation of specific neuronal subtypes (e.g., dopaminergic, cholinergic, GABAergic, and serotonergic) using sets of TFs.[35,54–56]

A large number of TFs are expressed in the SCN,[57] but systematic studies of embryonic development have revealed genetic distinctions between hypothalamic nuclei, including a specific genetic cascade that is critical for SCN formation.[14,37,58] VanDunk et al. (2011) showed that expression of a combination of developmental genes (Six3, Six6, and Fzd5, along with transient Rx) delineates where the SCN neuro epithelium will develop, distinguishing it from the embryonic telencephalon and diencephalon.[14] The loss of Rx induces early progenitor domains; however, Rx is not required for the specification of SCN neurons.[59] During SCN maturation the nucleus is divided into two regions, the ventrolateral core and the dorsomedial shell.[13] The formation of these functional subregions results from regional and temporal differences in cell proliferation, which themselves result from differential responses to developmental signals (e.g., morphogens).[14] Previous reports suggest that observation of mouse SCN at E12.5/13.5 indicate Lhx1 and Dlx2 expression in the developmental SCN marks the proliferative areas of postmitotic SCN neurons.[60] Altogether, the combination of Six3/Six6/Dlx2 and Lhx1 has been hypothesized as vital TFs of postmitotic SCN neurogenesis.[14] Whether this TF combination is sufficient to induce the differentiation of SCN neurons remains unknown.

In this study, we show that MEFs can be directly converted into neuronal subtypes with features of SCN neurons. Our differentiation protocol involves the expression of TFs and culture conditions used to produce iNs, as well as the expression of four TFs that act during SCN development. Surprisingly, this approach did not simply add SCN features to iNs, but iN-SCNTFs instead exhibited distinct features in terms of neurotransmitter expression and morphology. Most iNs generated here were glutamatergic and NeuN-positive. NeuN-positive neurons are found in nearly all brain regions, but NeuN is largely absent from several neuronal cell types, including cerebellar Purkinje cells, olfactory mitral cells, and SCN neurons.[61–63] Further, SCN neurons express GABA, VIP, and AVP. Consistent with this, very few iN-SCNTFs expressed NeuN, and they were predominantly GABAergic. We also found both AVP- and VIP-positive iN-SCNTFs. In fact, VIP-expressing neurons were

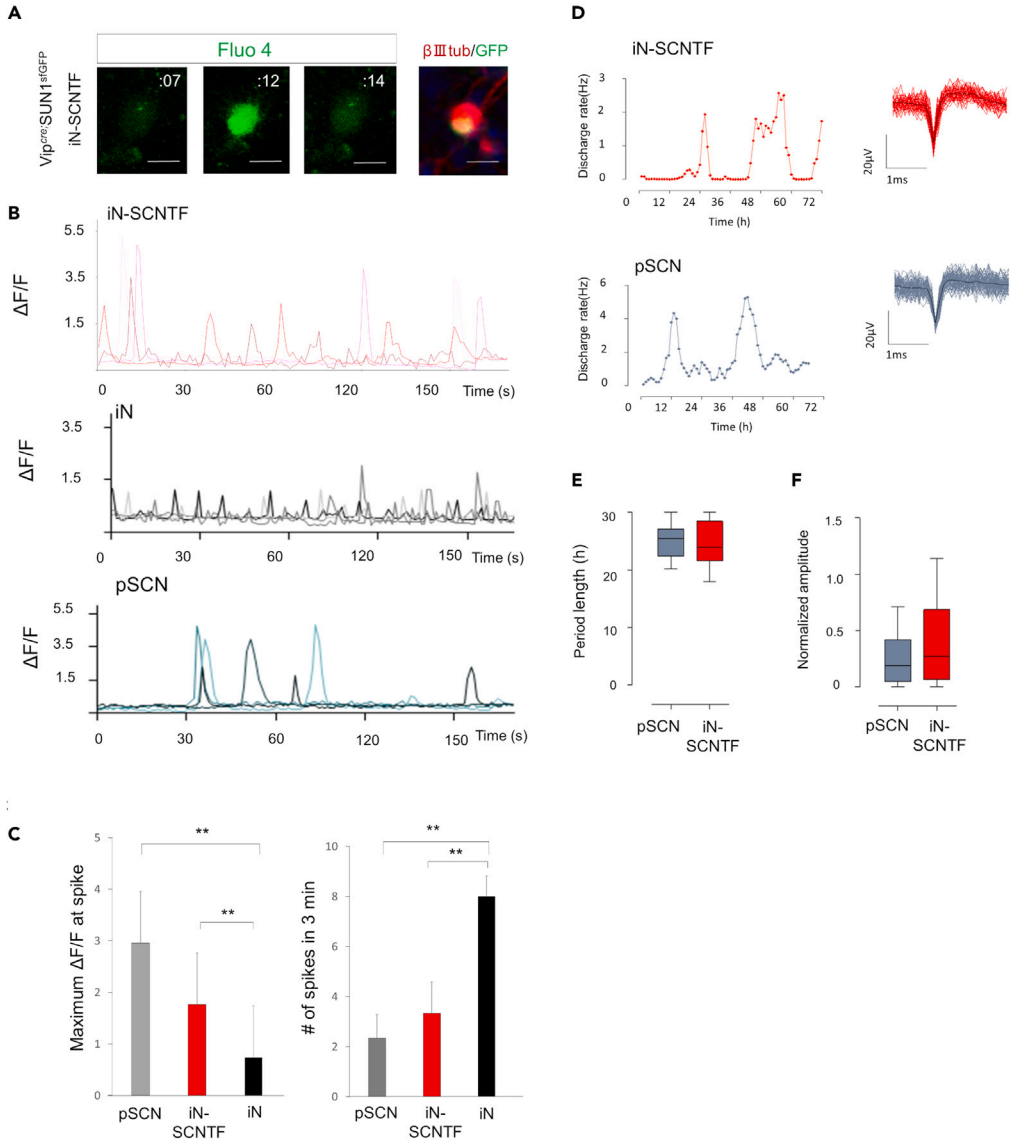

Figure 5. Electrophysiological activity to generate circadian rhythm in iN-SCNTF

(A) Representative images from time-lapse calcium imaging (Fluo4, green) of iN-SCNTF from Vip^{cre};Sun1^{sfGFP} mouse fibroblasts at time course (left 3 panels) and representative immunofluorescence image of the measured iN-SCNTF (βIII-tublin; red, GFP; green). Scale bars: 10μm.

(B) Three individual traces of calcium transients represented as change in fluorescence/minimum fluorescence (ΔF/F min) over time of iN-SCNTF (top panel), iN (middle panel) and primary SCN neurons (bottom panel).

(C) Quantitative analysis of neuronal activities in iN-SCNTF including maximum ΔF/F value in spikes (left) and the number of spikes in observation (right) were shown. There was a significant difference in the maximum ΔF/F between iN and iN-SCNTF (**$p < 0.001$, Student's t test), or iN and pSCN (**$p < 0.001$, Student's t test), but there was no significant difference between iN-SCNTF and pSCN ($p = 0.0697$, Student's t test). There was a significant difference in the number of spikes in 3 min (spike rhythm) between iN and iN-SCNTF (**$p = 0.0114$, Student's t test), or iN and pSCN (**$p = 0.0030$, Student's t test), but there was no significant differences between iN-SCNTF and pSCN ($p = 0.4169$, Student's t test).

(D) A multi-microelectrode arrays analysis (MEAA) recorded individual electroactivities in iN-SCNTF and primary SCN neurons (pSCN).

(E) MEAA showed period length of electroactivities in primary SCN neurons and iN-SCNTF. Period (h): $p = 0.782$, ns, Mann-Whitney test, pSCN n = 28 and iN-SCNTF n = 35 (from 3 independent experiments/plates).

(F) MEAA showed normalized amplitude of electroactivities in primary SCN neurons and iN-SCNTF. Normalized amplitude: $p = 0.074$, ns, Mann Whitney test, pSCN n = 28 and iN-SCNTF n = 35 (from 3 independent experiments/plates).

the most abundant in mouse iN-SCNTFs. VIP neurons are in the ventrolateral part of the SCN, exhibiting robust circadian time-keeping properties.[64] Concerning morphology, in particular dendritic branching patterns, light and electron microscopy studies have shown that SCN neurons are predominantly bipolar or multipolar, with a small number of monopolar cells.[65–67] Unlike iNs, which were predominantly unipolar, our iN-SCNTFs showed a greater proportion of bipolar or multipolar neurons besides unipolar neurons. Cell autonomous rhythms in SCN neurons generates a ~24-h rhythms in body activities. In the analysis of immortalized SCN cell lines, cells exhibit circadian rhythms in gene expression rhythms in many neuronal and non-neuronal cell types.[49] SCN neurons also have distinct characteristics of calcium transients and a ~24-h rhythm in firing pattern. These were also seen for iN-SCNTFs. However, no spontaneous firing pattern was observed in iNs, making evaluation difficult. Further analysis using living-cell sorting of highly purified Vip-expressing neurons from the iNs on MEAA would help our understanding on robustness and integrated rhythmic activities of iNs with Vip and GAD65/67 expression. There are important limitations to our approach. When we expressed the four TFs in MEFs, resulting neurons were mostly VIP-positive with a few AVP neurons. Although our TF cocktail is thought to have contributed primarily to the differentiation of Vip-expressing neurons, future studies, including a verification of the similarity of iN-SCNTF to the characteristics of the entire SCN neuron by single-cell transcriptome analysis using neuronal cell sorting and an analysis of clock function using luciferase reporter or time course single-cell analysis in iNs would provide more in-depth information.[68] In human fibroblasts, these same TFs, which were based on sequences in human, induced only a small number of VIP-positive iN-SCNTFs. Since very few VIP-expressing neurons were observed in human iN-SCNTFs, the protocol for iN-SCNTF differentiation and maturation must be further refined. With further refinement, it is clear that TFs involved in SCN organogenesis can be used in neuronal reprogramming protocols to generate iN-SCNTFs and help establish *in vitro* models of human circadian clock. In this study, we selected four TFs based on 15 TFs from mouse SCN specific TFs. Although there are practical limitations, consideration should be given to the applicability of TF combinations to humans and the effects of other TFs in SCN neurogenesis.

A recent study analyzed a three-dimensional reconstruction of the mouse SCN at single-cell resolution, defining the spatial arrangement of neuronal subtypes in the SCN.[68] While the functional relevance of these spatial arrangements is currently unclear, we anticipate the identification of developmental genes important for generating the elaborate three-dimensional structure of the SCN. These genes will likely aid in generating SCN-organoids with defined arrangements of SCN neuronal and non-neuronal cells. Interestingly, their single-cell resolution also showed *Six3* and *Six6* were notably enriched in SCN neurons, compared with non-SCN neurons, and Lhx1 was enriched in Vip positive subtypes, supporting our results.[68]

In conclusion, we used TFs important for SCN development to reprogram fibroblasts into neurons. INs that express *Six3*, *Six6*, *Lhx1*, and *Dlx2* exhibit similar characteristics of Vip-expressing neuronal subtype in the SCN, including morphology and neuropeptide expression, suggesting the importance of these TFs for SCN development. Our results will help establish *in vitro* models of circadian rhythm disorders, with the end goal of developing therapies for restoring SCN function.

Limitations of the study

In this study, we used 4 particularly important TFs from 15 candidate TFs in the SCN development for iN-SCNTFs induction, but the roles of the remaining TFs in SCN neurogenesis should be comprehensively investigated. Future investigation including transcriptome analysis after isolating neurons through cell sorting would provide interesting details of neurological properties and electrophysiological functions of the induced iN-SCNTF.

STAR★METHODS

Detailed methods are provided in the online version of this paper and include the following:

- KEY RESOURCES TABLE
- RESOURCE AVAILABILITY
  - Lead contact
  - Materials availability
  - Data and code availability
- EXPERIMENTAL MODEL AND SUBJECT DETAILS
  - Animals
- METHOD DETAILS
  - Culture and induction of fibroblasts to neurons
  - Vector design and generation of lentiviral particles
  - Immunofluorescence analysis
  - Time-lapse calcium imaging
  - Multi-electrode array recording
- QUANTIFICATION AND STATISTICAL ANALYSIS

SUPPLEMENTAL INFORMATION

Supplemental information can be found online at https://doi.org/10.1016/j.isci.2024.109051.

ACKNOWLEDGMENTS

We would like to thank Dr. David O'Keefe, Salk Institute for biological studies, for critically reviewing our manuscript. M.H. received Glenn fellowship from The Paul F. Glenn Center for Biology of Aging Research, and JSPS fellowship for study abroad from Japanese Society for Promotion of Science in Japan. S.P. is supported by the Wu Tsai Human Performance Alliance and the Joe and Clara Tsai Foundation.

AUTHOR CONTRIBUTIONS

Conceptualization: S.P. and M.H.; methodology: S.P., M.H., H.D.L, and L.S.M.; software: M.H. and L.S.M.; formal analysis: M.H. and L.S.M.; investigation: M.H., H.D.L., and L.S.M.; resources: M.H., H.D.L., and L.S.M.; data curation: M.H. and L.S.M.; writing – original draft: M.H., L.S.M., and S.P.; writing – review and editing: M.H., L.S.M., and S.P.

DECLARATION OF INTERESTS

The authors declare no competing interests.

Received: August 29, 2023
Revised: October 18, 2023
Accepted: January 23, 2024
Published: January 30, 2024

REFERENCES

1. Welsh, D.K., Takahashi, J.S., and Kay, S.A. (2010). Suprachiasmatic nucleus: cell autonomy and network properties. Annu. Rev. Physiol. *72*, 551–577. https://doi.org/10.1146/annurev-physiol-021909-135919.
2. Saper, C.B. (2013). The central circadian timing system. Curr. Opin. Neurobiol. *23*, 747–751. https://doi.org/10.1016/j.conb.2013.04.004.
3. Abrahamson, E.E., and Moore, R.Y. (2001). Suprachiasmatic nucleus in the mouse: retinal innervation, intrinsic organization and efferent projections. Brain Res. *916*, 172–191. https://doi.org/10.1016/s0006-8993(01)02890-6.
4. Lee, J.E., Atkins, N., Jr., Hatcher, N.G., Zamdborg, L., Gillette, M.U., Sweedler, J.V., and Kelleher, N.L. (2010). Endogenous peptide discovery of the rat circadian clock: a focused study of the suprachiasmatic nucleus by ultrahigh performance tandem mass spectrometry. Mol. Cell. Proteomics *9*, 285–297. https://doi.org/10.1074/mcp.M900362-MCP200.
5. Morin, L.P., Shivers, K.Y., Blanchard, J.H., and Muscat, L. (2006). Complex organization of mouse and rat suprachiasmatic nucleus. Neuroscience *137*, 1285–1297. https://doi.org/10.1016/j.neuroscience.2005.10.030.
6. Moore, R.Y., and Speh, J.C. (1993). GABA is the principal neurotransmitter of the circadian system. Neurosci. Lett. *150*, 112–116. https://doi.org/10.1016/0304-3940(93)90120-a.
7. Morin, L.P., and Blanchard, J.H. (2001). Neuromodulator content of hamster intergeniculate leaflet neurons and their projection to the suprachiasmatic nucleus or visual midbrain. J. Comp. Neurol. *437*, 79–90. https://doi.org/10.1002/cne.1271.
8. Ono, D., Honma, K.I., and Honma, S. (2021). Roles of Neuropeptides, VIP and AVP, in the Mammalian Central Circadian Clock. Front. Neurosci. *15*, 650154. https://doi.org/10.3389/fnins.2021.650154.
9. Ono, D., Honma, K.I., and Honma, S. (2021). GABAergic mechanisms in the suprachiasmatic nucleus that influence circadian rhythm. J. Neurochem. *157*, 31–41. https://doi.org/10.1111/jnc.15012.
10. Brown, T.M., Hughes, A.T., and Piggins, H.D. (2005). Gastrin-releasing peptide promotes suprachiasmatic nuclei cellular rhythmicity in the absence of vasoactive intestinal polypeptide-VPAC2 receptor signaling. J. Neurosci. *25*, 11155–11164. https://doi.org/10.1523/JNEUROSCI.3821-05.2005.
11. Maywood, E.S., Chesham, J.E., O'Brien, J.A., and Hastings, M.H. (2011). A diversity of paracrine signals sustains molecular circadian cycling in suprachiasmatic nucleus circuits. Proc. Natl. Acad. Sci. USA *108*, 14306–14311. https://doi.org/10.1073/pnas.1101767108.
12. Reghunandanan, V. (2020). Vasopressin in circadian function of SCN. J. Biosci. *45*, 140.
13. Altman, J., and Bayer, S.A. (1986). The development of the rat hypothalamus. Adv. Anat. Embryol. Cell Biol. *100*, 1–178.
14. VanDunk, C., Hunter, L.A., and Gray, P.A. (2011). Development, maturation, and necessity of transcription factors in the mouse suprachiasmatic nucleus. J. Neurosci. *31*, 6457–6467. https://doi.org/10.1523/JNEUROSCI.5385-10.2011.
15. Liu, R.Y., Unmehopa, U.A., Zhou, J.N., and Swaab, D.F. (2006). Glucocorticoids suppress vasopressin gene expression in human suprachiasmatic nucleus. J. Steroid Biochem. Mol. Biol. *98*, 248–253. https://doi.org/10.1016/j.jsbmb.2005.10.002.
16. Clark, D.D., Gorman, M.R., Hatori, M., Meadows, J.D., Panda, S., and Mellon, P.L. (2013). Aberrant development of the suprachiasmatic nucleus and circadian rhythms in mice lacking the homeodomain protein Six6. J. Biol. Rhythms *28*, 15–25. https://doi.org/10.1177/0748730412468084.
17. Hatori, M., Gill, S., Mure, L.S., Goulding, M., O'Leary, D.D.M., and Panda, S. (2014). Lhx1 maintains synchrony among circadian oscillator neurons of the SCN. Elife *3*, e03357. https://doi.org/10.7554/eLife.03357.
18. Vierbuchen, T., Ostermeier, A., Pang, Z.P., Kokubu, Y., Südhof, T.C., and Wernig, M. (2010). Direct conversion of fibroblasts to functional neurons by defined factors. Nature *463*, 1035–1041. https://doi.org/10.1038/nature08797.
19. Takahashi, K., and Yamanaka, S. (2006). Induction of pluripotent stem cells from mouse embryonic and adult fibroblast cultures by defined factors. Cell *126*, 663–676. https://doi.org/10.1016/j.cell.2006.07.024.
20. Pang, X.N. (2011). [Cell reprogramming: control key genes to obtain needed cells]. Zhongguo Yi Xue Ke Xue Yuan Xue Bao. *33*, 689–695.
21. Mertens, J., Marchetto, M.C., Bardy, C., and Gage, F.H. (2016). Evaluating cell reprogramming, differentiation and conversion technologies in neuroscience. Nat. Rev. Neurosci. *17*, 424–437. https://doi.org/10.1038/nrn.2016.46.
22. Panda, S. (2016). Circadian physiology of metabolism. Science *354*, 1008–1015. https://doi.org/10.1126/science.aah4967.
23. Hatori, M., Gronfier, C., Van Gelder, R.N., Bernstein, P.S., Carreras, J., Panda, S., Marks, F., Sliney, D., Hunt, C.E., Hirota, T., et al. (2017). Global rise of potential health hazards caused by blue light-induced circadian disruption in modern aging societies. NPJ Aging Mech. Dis. *3*, 9. https://doi.org/10.1038/s41514-017-0010-2.
24. Kecklund, G., and Axelsson, J. (2016). Health consequences of shift work and insufficient sleep. BMJ *355*, i5210. https://doi.org/10.1136/bmj.i5210.
25. Khachiyants, N., Trinkle, D., Son, S.J., and Kim, K.Y. (2011). Sundown syndrome in persons with dementia: an update. Psychiatry Investig. *8*, 275–287. https://doi.org/10.4306/pi.2011.8.4.275.
26. Boer, G.J., van Esseveldt, L.E., and Rietveld, W.J. (1998). Cellular requirements of suprachiasmatic nucleus transplants for restoration of circadian rhythm. Chronobiol. Int. *15*, 551–566. https://doi.org/10.3109/07420529808998707.
27. Ralph, M.R., Foster, R.G., Davis, F.C., and Menaker, M. (1990). Transplanted suprachiasmatic nucleus determines circadian period. Science *247*, 975–978. https://doi.org/10.1126/science.2305266.
28. Pickard, G.E., Sollars, P.J., Rinchik, E.M., Nolan, P.M., and Bucan, M. (1995). Mutagenesis and behavioral screening for altered circadian activity identifies the mouse mutant, Wheels. Brain Res. *705*, 255–266.

https://doi.org/10.1016/0006-8993(95)01171-4.
29. Sollars, P.J., and Pickard, G.E. (1998). Restoration of circadian behavior by anterior hypothalamic grafts containing the suprachiasmatic nucleus: graft/host interconnections. Chronobiol. Int. *15*, 513–533. https://doi.org/10.3109/07420529808998705.
30. Meyer-Bernstein, E.L., Jetton, A.E., Matsumoto, S.I., Markuns, J.F., Lehman, M.N., and Bittman, E.L. (1999). Effects of suprachiasmatic transplants on circadian rhythms of neuroendocrine function in golden hamsters. Endocrinology *140*, 207–218. https://doi.org/10.1210/endo.140.1.6428.
31. Vasan, L., Park, E., David, L.A., Fleming, T., and Schuurmans, C. (2021). Direct Neuronal Reprogramming: Bridging the Gap Between Basic Science and Clinical Application. Front. Cell Dev. Biol. *9*, 681087. https://doi.org/10.3389/fcell.2021.681087.
32. Ladewig, J., Mertens, J., Kesavan, J., Doerr, J., Poppe, D., Glaue, F., Herms, S., Wernet, P., Kögler, G., Müller, F.J., et al. (2012). Small molecules enable highly efficient neuronal conversion of human fibroblasts. Nat. Methods *9*, 575–578. https://doi.org/10.1038/nmeth.1972.
33. Mertens, J., Paquola, A.C.M., Ku, M., Hatch, E., Böhnke, L., Ladjevardi, S., McGrath, S., Campbell, B., Lee, H., Herdy, J.R., et al. (2015). Directly Reprogrammed Human Neurons Retain Aging-Associated Transcriptomic Signatures and Reveal Age-Related Nucleocytoplasmic Defects. Cell Stem Cell *17*, 705–718. https://doi.org/10.1016/j.stem.2015.09.001.
34. Caiazzo, M., Dell'Anno, M.T., Dvoretskova, E., Lazarevic, D., Taverna, S., Leo, D., Sotnikova, T.D., Menegon, A., Roncaglia, P., Colciago, G., et al. (2011). Direct generation of functional dopaminergic neurons from mouse and human fibroblasts. Nature *476*, 224–227. https://doi.org/10.1038/nature10284.
35. Vadodaria, K.C., Mertens, J., Paquola, A., Bardy, C., Li, X., Jappelli, R., Fung, L., Marchetto, M.C., Hamm, M., Gorris, M., et al. (2016). Generation of functional human serotonergic neurons from fibroblasts. Mol. Psychiatry *21*, 49–61. https://doi.org/10.1038/mp.2015.161.
36. Su, A.I., Wiltshire, T., Batalov, S., Lapp, H., Ching, K.A., Block, D., Zhang, J., Soden, R., Hayakawa, M., Kreiman, G., et al. (2004). A gene atlas of the mouse and human protein-encoding transcriptomes. Proc. Natl. Acad. Sci. USA *101*, 6062–6067. https://doi.org/10.1073/pnas.0400782101.
37. Gray, P.A., Fu, H., Luo, P., Zhao, Q., Yu, J., Ferrari, A., Tenzen, T., Yuk, D.I., Tsung, E.F., Cai, Z., et al. (2004). Mouse brain organization revealed through direct genome-scale TF expression analysis. Science *306*, 2255–2257. https://doi.org/10.1126/science.1104935.
38. Bedont, J.L., LeGates, T.A., Slat, E.A., Byerly, M.S., Wang, H., Hu, J., Rupp, A.C., Qian, J., Wong, G.W., Herzog, E.D., et al. (2014). Lhx1 controls terminal differentiation and circadian function of the suprachiasmatic nucleus. Cell Rep. *7*, 609–622. https://doi.org/10.1016/j.celrep.2014.03.060.
39. Pandolfi, E.C., Breuer, J.A., Nguyen Huu, V.A., Talluri, T., Nguyen, D., Lee, J.S., Hu, R., Bharti, K., Skowronska-Krawczyk, D., Gorman, M.R., et al. (2020). The Homeodomain Transcription Factors Vax1 and Six6 Are Required for SCN Development and Function. Mol. Neurobiol. *57*, 1217–1232. https://doi.org/10.1007/s12035-019-01781-9.
40. Hoffmann, H.M., Meadows, J.D., Breuer, J.A., Yaw, A.M., Nguyen, D., Tonsfeldt, K.J., Chin, A.Y., Devries, B.M., Trang, C., Oosterhouse, H.J., et al. (2021). The transcription factors SIX3 and VAX1 are required for suprachiasmatic nucleus circadian output and fertility in female mice. J. Neurosci. Res. *99*, 2625–2645. https://doi.org/10.1002/jnr.24864.
41. Hofman, M.A., Fliers, E., Goudsmit, E., and Swaab, D.F. (1988). Morphometric analysis of the suprachiasmatic and paraventricular nuclei in the human brain: sex differences and age-dependent changes. J. Anat. *160*, 127–143.
42. Welsh, D.K., Logothetis, D.E., Meister, M., and Reppert, S.M. (1995). Individual neurons dissociated from rat suprachiasmatic nucleus express independently phased circadian firing rhythms. Neuron *14*, 697–706. https://doi.org/10.1016/0896-6273(95)90214-7.
43. DeWoskin, D., Myung, J., Belle, M.D.C., Piggins, H.D., Takumi, T., and Forger, D.B. (2015). Distinct roles for GABA across multiple timescales in mammalian circadian timekeeping. Proc. Natl. Acad. Sci. USA *112*, E3911–E3919. https://doi.org/10.1073/pnas.1420753112.
44. Mo, A., Mukamel, E.A., Davis, F.P., Luo, C., Henry, G.L., Picard, S., Urich, M.A., Nery, J.R., Sejnowski, T.J., Lister, R., et al. (2015). Epigenomic Signatures of Neuronal Diversity in the Mammalian Brain. Neuron *86*, 1369–1384. https://doi.org/10.1016/j.neuron.2015.05.018.
45. Ono, D., Honma, K.I., Yanagawa, Y., Yamanaka, A., and Honma, S. (2018). Role of GABA in the regulation of the central circadian clock of the suprachiasmatic nucleus. J. Physiol. Sci. *68*, 333–343. https://doi.org/10.1007/s12576-018-0604-x.
46. Badger, J.L., Cordero-Llana, O., Hartfield, E.M., and Wade-Martins, R. (2014). Parkinson's disease in a dish - Using stem cells as a molecular tool. Neuropharmacology *76*, 88–96. https://doi.org/10.1016/j.neuropharm.2013.08.035.
47. Kokaia, Z., Tornero, D., and Lindvall, O. (2017). Transplantation of reprogrammed neurons for improved recovery after stroke. Prog. Brain Res. *231*, 245–263. https://doi.org/10.1016/bs.pbr.2016.11.013.
48. Honma, S., Ono, D., Suzuki, Y., Inagaki, N., Yoshikawa, T., Nakamura, W., and Honma, K.I. (2012). Suprachiasmatic nucleus: cellular clocks and networks. Prog. Brain Res. *199*, 129–141. https://doi.org/10.1016/B978-0-444-59427-3.00029-0.
49. Earnest, D.J., Liang, F.Q., DiGiorgio, S., Gallagher, M., Harvey, B., Earnest, B., and Seigel, G. (1999). Establishment and characterization of adenoviral E1A immortalized cell lines derived from the rat suprachiasmatic nucleus. J. Neurobiol. *39*, 1–13. https://doi.org/10.1002/(sici)1097-4695(199904)39:1<1::aid-neu1>3.0.co;2-f.
50. Vogelbaum, M.A., Galef, J., and Menaker, M. (1993). Factors determining the restoration of circadian behavior by hypothalamic transplants. J. Neural Transplant. Plast. *4*, 239–256. https://doi.org/10.1155/NP.1993.239.
51. Sollars, P.J., and Pickard, G.E. (1995). Vasoactive intestinal peptide efferent projections of the suprachiasmatic nucleus in anterior hypothalamic transplants: correlation with functional restoration of circadian behavior. Exp. Neurol. *136*, 1–11. https://doi.org/10.1006/exnr.1995.1078.
52. Tousson, E., and Meissl, H. (2004). Suprachiasmatic nuclei grafts restore the circadian rhythm in the paraventricular nucleus of the hypothalamus. J. Neurosci. *24*, 2983–2988. https://doi.org/10.1523/JNEUROSCI.5044-03.2004.
53. Aguilar-Roblero, R., Morin, L.P., and Moore, R.Y. (1994). Morphological correlates of circadian rhythm restoration induced by transplantation of the suprachiasmatic nucleus in hamsters. Exp. Neurol. *130*, 250–260. https://doi.org/10.1006/exnr.1994.1203.
54. Caiazzo, M., Giannelli, S., Valente, P., Lignani, G., Carissimo, A., Sessa, A., Colasante, G., Bartolomeo, R., Massimino, L., Ferroni, S., et al. (2015). Direct conversion of fibroblasts into functional astrocytes by defined transcription factors. Stem Cell Rep. *4*, 25–36. https://doi.org/10.1016/j.stemcr.2014.12.002.
55. Liu, M.L., Zang, T., Zou, Y., Chang, J.C., Gibson, J.R., Huber, K.M., and Zhang, C.L. (2013). Small molecules enable neurogenin 2 to efficiently convert human fibroblasts into cholinergic neurons. Nat. Commun. *4*, 2183. https://doi.org/10.1038/ncomms3183.
56. Yang, N., Chanda, S., Marro, S., Ng, Y.H., Janas, J.A., Haag, D., Ang, C.E., Tang, Y., Flores, Q., Mall, M., et al. (2017). Generation of pure GABAergic neurons by transcription factor programming. Nat. Methods *14*, 621–628. https://doi.org/10.1038/nmeth.4291.
57. Takahashi, J.S. (2017). Transcriptional architecture of the mammalian circadian clock. Nat. Rev. Genet. *18*, 164–179. https://doi.org/10.1038/nrg.2016.150.
58. Sládek, M., Sumová, A., Kováciková, Z., Bendová, Z., Laurinová, K., and Illnerová, H. (2004). Insight into molecular core clock mechanism of embryonic and early postnatal rat suprachiasmatic nucleus. Proc. Natl. Acad. Sci. USA *101*, 6231–6236. https://doi.org/10.1073/pnas.0401149101.
59. Liu, W., Lagutin, O., Swindell, E., Jamrich, M., and Oliver, G. (2010). Neuroretina specification in mouse embryos requires Six3-mediated suppression of Wnt8b in the anterior neural plate. J. Clin. Invest. *120*, 3568–3577. https://doi.org/10.1172/JCI43219.
60. Kabrita, C.S., and Davis, F.C. (2008). Development of the mouse suprachiasmatic nucleus: determination of time of cell origin and spatial arrangements within the nucleus. Brain Res. *1195*, 20–27. https://doi.org/10.1016/j.brainres.2007.12.020.
61. Kumar, S.S., and Buckmaster, P.S. (2007). Neuron-specific nuclear antigen NeuN is not detectable in gerbil subtantia nigra pars reticulata. Brain Res. *1142*, 54–60. https://doi.org/10.1016/j.brainres.2007.01.027.
62. Mullen, R.J., Buck, C.R., and Smith, A.M. (1992). NeuN, a neuronal specific nuclear protein in vertebrates. Development *116*, 201–211. https://doi.org/10.1242/dev.116.1.201.
63. Morin, L.P., Hefton, S., and Studholme, K.M. (2011). Neurons identified by NeuN/Fox-3 immunoreactivity have a novel distribution in the hamster and mouse suprachiasmatic nucleus. Brain Res. *1421*, 44–51. https://doi.org/10.1016/j.brainres.2011.09.015.
64. Mazuski, C., Abel, J.H., Chen, S.P., Hermanstyne, T.O., Jones, J.R., Simon, T.,

Doyle, F.J., 3rd, and Herzog, E.D. (2018). Entrainment of Circadian Rhythms Depends on Firing Rates and Neuropeptide Release of VIP SCN Neurons. Neuron *99*, 555–563.e5. https://doi.org/10.1016/j.neuron.2018.06.029.

65. Pennartz, C.M., De Jeu, M.T., Geurtsen, A.M., Sluiter, A.A., and Hermes, M.L. (1998). Electrophysiological and morphological heterogeneity of neurons in slices of rat suprachiasmatic nucleus. J. Physiol. *506*, 775–793. https://doi.org/10.1111/j.1469-7793.1998.775bv.x.
66. Van den Pol, A.N. (1980). The hypothalamic suprachiasmatic nucleus of rat: intrinsic anatomy. J. Comp. Neurol. *191*, 661–702. https://doi.org/10.1002/cne.901910410.
67. Ren, D., and Miller, J.D. (2003). Primary cell culture of suprachiasmatic nucleus. Brain Res. Bull. *61*, 547–553. https://doi.org/10.1016/s0361-9230(03)00193-x.
68. Wen, S., Ma, D., Zhao, M., Xie, L., Wu, Q., Gou, L., Zhu, C., Fan, Y., Wang, H., and Yan, J. (2020). Spatiotemporal single-cell analysis of gene expression in the mouse suprachiasmatic nucleus. Nat. Neurosci. *23*, 456–467. https://doi.org/10.1038/s41593-020-0586-x.
69. Chou, S.J., Babot, Z., Leingärtner, A., Studer, M., Nakagawa, Y., and O'Leary, D.D.M. (2013). Geniculocortical input drives genetic distinctions between primary and higher-order visual areas. Science *340*, 1239–1242. https://doi.org/10.1126/science.1232806.
70. Wu, G., Anafi, R.C., Hughes, M.E., Kornacker, K., and Hogenesch, J.B. (2016). MetaCycle: an integrated R package to evaluate periodicity in large scale data. Bioinformatics *32*, 3351–3353. https://doi.org/10.1093/bioinformatics/btw405.
71. Yang, R., and Su, Z. (2010). Analyzing circadian expression data by harmonic regression based on autoregressive spectral estimation. Bioinformatics *26*, i168–i174. https://doi.org/10.1093/bioinformatics/btq189.
72. Hughes, M.E., Hogenesch, J.B., and Kornacker, K. (2010). JTK_CYCLE: an efficient nonparametric algorithm for detecting rhythmic components in genome-scale data sets. J. Biol. Rhythms *25*, 372–380. https://doi.org/10.1177/0748730410379711.
73. Glynn, E.F., Chen, J., and Mushegian, A.R. (2006). Detecting periodic patterns in unevenly spaced gene expression time series using Lomb-Scargle periodograms. Bioinformatics *22*, 310–316. https://doi.org/10.1093/bioinformatics/bti789.

STAR★METHODS

KEY RESOURCES TABLE

REAGENT or RESOURCE	SOURCE	IDENTIFIER
Antibodies		
Mouse anti Beta-III-tubulin	BioLegend	Cat#MMS-435P; N/A
Rabbit anti Beta-III-tubulin	BioLegend	Cat#802001; RRID:AB_2564645
Chicken anti Map2	Abcam	Cat#ab5392; RRID:AB_2138153
Mouse anti Map2ab	Sigma-Aldrich	Cat# M1406; RRID:AB_477171
Mouse anti NeuN	EMD Millipore	Cat#MAB377; RRID:AB_2298772
Rabbit anti NeuN	Cell Signaling	Cat#24307T; N/A
Rabbit anti vGlut1	Synaptic Systems	Cat#135302; RRID:AB_887877
Rabbit anti γ-Aminobutyric acid	Sigma Aldrich	Cat#A2052; RRID:AB_477652
Chicken anti GFP	Gage laboratory	N/A
Rabbit anti GFP	Cell Signaling	Cat#2956; RRID:AB_1196615
Rabbit anti GAD65	EMD Millipore	Cat.# ABN10; N/A
Rabbit anti GAD65/67	EMD MIllipore	Cat.#AB1511; RRID:AB_90715
Mouse anti GAD67	Abcam	Ab26116; RRID:AB_448990
Rabbit anti Vip	ImmunoStar	Cat#20077; RRID:AB_572270
Alexa Fluor 488-conjugated Donkey Anti Rabbit IgG	Thermo Fisher Scientific	Cat#A-21206; RRID:AB_2535792
Alexa Fluor 647-conjugated Donkey Anti Rabbit IgG	Thermo Fisher Scientific	Cat#A-31573; RRID:AB_2536183
Alexa Fluor 488-conjugated Donkey Anti Mouse IgG	Thermo Fisher Scientific	Cat#A-21202; RRID:AB_141607
Alexa Fluor 647-conjugated Donkey Anti Mouse IgG	Thermo Fisher Scientific	Cat#A-31571; RRID:AB_162542
Cy3-conjugated Donkey Anti-Mouse IgG	Jackson ImmunoRes.	Cat#711-165-151; N/A
Cy3-conjugated Donkey Anti-Rabbit IgG	Jackson ImmunoRes.	Cat#711-165-152; RRID:AB_2307443
Alexa Fluor 488-conjugated Donkey Anti Chicken IgY	Gage Laboratory	N/A
Cy3-conjugated Donkey Anti Chicken IgY	Gage Laboratory	N/A
Alexa Fluor 647-conjugated Donkey Anti Chicken IgY	Gage Laboratory	N/A
Bacterial and virus strains		
NEB Stable Competent *E. coli*	New England Biolabs	Cat#C3040H
Chemicals, peptides, and recombinant proteins		
B-27 supplement	Thermo Fisher Scientific	Cat#17504044
N2 supplement	Thermo Fisher Scientific	Cat#17502048
Dibutyryl-cyclic-AMP	Sigma Aldrich	Cat#sc-201567B
Recombinant Noggin	Preprotech	Cat#6057NG
CHIR99021	LC Laboratories	Cat#C-6556
LDN-193189	Cayman Chemicals	Cat#19396
A83-1	Santa Cruz Biotech	Cat#K1119
Forskolin	LC Laboratories	Cat#F-9929
SB-431542	Cayman Chemicals	Cat#431543
Poly-L-ornithine coating reagent	Sigma Aldrich	Cat#A-004-C
Recombinant human GDNF	R&D Biosystems	Cat#212-GD
Recombinant human BDNF	R&D Biosystems	Cat#248-BDB
Doxycycline	Sigma Aldrich	Cat#089M4004V
Triton X-100 reagent	Sigma Aldrich	Cat#X100
DAPI fluorescence reagent for DNA	Sigma Aldrich	Cat#D8417

(*Continued on next page*)

Continued

REAGENT or RESOURCE	SOURCE	IDENTIFIER
TURBO DNase for NGS library preparation	Ambion	Cat#AM2238
DNase for cell culture	Roche	Cat#4716728001
TruSeq Stranded mRNA Sample Prep kit	Illumina	Cat#20020594
SYBR Green I for qPCR	Life Technologies	Cat#S7563
SuperScript III First-Strand Synthesis System	Thermo Fisher Scientific	Cat#18080051
Non-Essential Amino Acids (NEAA) supplement	Thermo Fisher Scientific	Cat#M7145
cOmplete EDTA-free Protease Inhibitor Cocktail	Roche	Cat#11836170001
KOSR	Thermo Fisher Scientific	Cat#10828028
Critical commercial assays		
Fluo-4 Calcium Imaging Kit	Thermo Fisher Scientific	F10489
Experimental models: Cell lines		
Mouse embryonic Fibroblasts	This study	N/A
Human Fibroblasts (BJ cell line)	ATCC	CRL-2522; RRID:CVCL_3653
Oligonucleotides		
Synthesized sequences for DLX2: GCGGCCGCCGCCACCATGGACTAC AAGGATGACGACGATAAGACCGGCGTGTTCGACAGCCTGGTGGCC GATATGCACTCCACCCAGATCGCCGCCAGCTCCACATACCACCAGC ACCAGCAGCCACCTTCCGGAGGAGGAGCAGGCCCTGGCGGCAACT CTAGCTCCTCTAGCTCCCTGCACAAGCCTCAGGAGTCTCCAACCCTG CCCGTGAGCACCGCCACAGACTCTAGCTACTATACAAATCAGCAGC ACCCAGCAGGCGGCGGAGGAGGAGGAGGAAGCCCCTATGCCCAC ATGGGCTCCTACCAGTATCAGGCCTCTGGCCTGAACAATGTGCCCT ACTCTGCCAAGTCCTCTTATGACCTGGGCTACACCGCCGCCTACAC AAGCTATGCCCCATACGGCACAAGCTCCTCTCCCGCCAACAATGAG CCTGAGAAGGAGGATCTGGAGCCCGAGATCAGGATCGTGAACGGC AAGCCTAAGAAGGTGCGGAAGCCAAGAACCATCTATAGCTCCTTCC AGCTGGCCGCCCTGCAGCGGAGATTTCAGAAGACACAGTACCTGG CCCTGCCTGAGAGGGCAGAGCTGGCAGCCTCCCTGGGCCTGACCC AGACACAGGTGAAGATCTGGTTCCAGAATAGGCGCAGCAAGTTTAA GAAGATGTGGAAGAGCGGAGAGATCCCATCCGAGCAGCACCCCGG CGCATCTGCCAGCCCACCATGCGCCAGCCCTCCAGTGTCCGCCCC AGCATCTTGGGATTTCGGCGTGCCTCAGCGGATGGCCGGCGGAGG AGGCCCTGGCTCCGGAGGCTCTGGAGCAGGCTCTAGCGGCTCCTC TCCTAGCTCCGCCGCATCCGCCTTTCTGGGAAACTATCCCTGGTATC ACCAGACCTCCGGATCCGCCAGCCACCTGCAGGCAACAGCACCTCT GCTGCACCCAACCCAGACACCCCAGCCTCACCATCATCACCACCAC CACGGCGGAGGAGGCGCCCCAGTGAGCGCCGGCACCATCTTTTGA ACGCGT	This study	N/A
Synthesized sequences for LHX1: GCGGCCGCCGCCACCATGGACTACA AGGATGACGACGATAAGGTGCATTGCGCTGGCTGTAAAAGACCTATT CTGGATAGATTCCTGCTGAACGTGCTGGACCGGGCTTGGCATGTGAA ATGCGTGCAGTGCTGTGAGTGCAAGTGTAACCTGACAGAGAAATGTT TCAGCCGGGAAGGAAAGCTGTACTGTAAGAACGACTTCTTTAGATGC TTCGGCACTAAGTGCGCTGGATGTGCACAGGGCATCAGCCCCTCCGA TCTGGTGCGGAGAGCCAGGTCTAAGGTCTTCCACCTGAACTGCTTTA CCTGTATGATGTGCAACAAGCAGCTGAGCACAGGCGAGGAACTGTA CATCATTGACGAGAACAAGTTCGTGTGCAAAGAAGATTATCTGTCTAA CAGCTCCGTCGCTAAGGAGAATAGCCTGCATTCCGCAACCACAGGC AGTGACCCTTCTCTGAGTCCAGACTCTCAGGATCCAAGTCAGGACGA TGCAAAGGACTCAGAAAGCGCCAACGTGTCAGATAAAGAGGCCGGG	This study	N/A

(*Continued on next page*)

Continued

REAGENT or RESOURCE	SOURCE	IDENTIFIER
AGCAACGAAAATGACGATCAGAATCTGGGGGCAAAAAGGCGCGGAC CCCGGACTACCATTAAGGCCAAACAGCTGGAGACCCTGAAGGCCGC TTTCGCAGCCACACCCAAACCTACTAGGCACATCCGCGAGCAGCTGG CTCAGGAAACAGGGCTGAACATGAGAGTGATCCAGGTCTGGTTTCAG AATCGACGGAGCAAGGAAAGAAGGATGAAACAGCTGTCCGCCCTGG GCGCCCGGCGGCACGCCTTCTTCCGCAGCCCACGGAGAATGCGACC CCTGGTGGACCGCCTGGAGCCTGGCGAACTGATCCCCAACGGGCCT TTCTCCTTTTACGGAGACTATCAGTCTGAGTACTATGGCCCTGGCGGG AATTATGATTTCTTTCCACAGGGGCCCCCTTCTAGTCAGGCCCAGACT CCCGTGGATCTGCCATTCGTCCCCTCAAGCGGACCAAGCGGGACCC CTCTGGGAGGCCTGGAGCACCCACTGCCCGGCCACCATCCTTCCTCT GAAGCCCAGCGGTTCACCGACATTCTGGCTCACCCACCCGGAGATTC CCCTTCTCCAGAGCCCTCCCTGCCTGGCCCACTGCATAGTATGTCAG CTGAAGTGTTCGGGCCCAGTCCTCCCTTCAGCAGCCTGTCAGTCAAT GGGGGAGCATCCTATGGGAATCACCTGTCACATCCACCTGAAATGAA CGAAGCCGCCGTCTGGTAAACGCGT,		
Synthesized sequences for SIX6: GCGGCCGCCGCCACCATGGACTACAAGGATGACGACGATAAGTTCC AGCTGCCCATCCTGAACTTTAGCCCTCAGCAGGTGGCAGGCGTGTGC GAGACCCTGGAGGAGTCCGGCGACGTGGAGCGGCTGGGCAGATTC CTGTGGTCTCTGCCAGTGGCACCAGCAGCATGTGAGGCCCTGAACA AGAATGAGAGCGTGCTGAGGGCCCGCGCCATCGTGGCATTCCACGG CGGCAACTACAGGGAGCTGTATCACATCCTGGAGAATCACAAGTTTA CAAAGGAGTCCCACGCAAAGCTGCAGGCCCTGTGGCTGGAGGCCCA CTACCAGGAGGCAGAGAAGCTGCGGGGCAGACCTCTGGGACCAGT GGACAAGTATAGGGTGCGCAAGAAGTTCCCCCTGCCTCGCACCATCT GGGATGGCGAGCAGAAGACCCACTGCTTTAAGGAGCGGACAAGAAA CCTGCTGCGGGAGTGGTATCTGCAGGATCCATATCCCAATCCTTCTAA GAAGAGAGAGCTGGCACAGGCAACAGGACTGACCCCTACACAAGTG GGCAACTGGTTTAAGAATCGGAGACAGAGGGACAGGGCTGCCGCCG CCAAGAATAGGCTGCAGCAGCAGGTGCTGTCCCAGGGATCTGGCAG GGCCCTGAGGGCAGAGGGCGATGGCACCCCAGAGGTGCTGGGAGT GGCCACATCTCCAGCAGCCAGCCTGAGCAGCAAGGCAGCCACCAGC GCCATCTCCATCACATCTAGCGACTCCGAGTGTGACATCTGAACGCGT	This study	N/A
Synthesized sequences for SIX3: GCGGCCGCCGCCACCATGGACTACAAGGATGACGACGATAAGGTCT TCCGATCACCACTGGACCTGTATTCTTCACATTTTCTGCTGCCCAACTT CGCCGATTCACACCATAGGAGTATTCTGCTGGCTAGCTCCGGCGGGG GAAACGGAGCAGGAGGAGGAGGAGGAGCTGGAGGCGGGAGTGGA GGCGGGAATGGCGCCGGAGGCGGGGGAGCTGGCGGGGCAGGAGG CGGGGGAGGCGGGGGATCTAGGGCCCCCCCTGAGGAACTGAGTAT GTTCCAGCTGCCTACTCTGAACTTTAGCCCAGAGCAGGTGGCCTCCG TCTGCGAAACACTGGAGGAAACTGGCGACATCGAAAGGCTGGGGCG CTTCCTGTGGTCCCTGCCTGTGGCCCCAGGCGCTTGTGAGGCAATCA ATAAGCACGAATCTATTCTGAGGGCCCGCGCTGTGGTCGCCTTCCATA CAGGCAACTTTAGGGATCTGTACCACATTCTGGAGAACCATAAGTTTA CTAAGGAAAGCCACGGCAAGCTGCAGGCCATGTGGCTGGAGGCTCA TTACCAGGAGGCAGAAAAGCTGCGAGGACGGCCCCTGGGACCTGTG GACAAATATAGAGTCAGGAAGAAATTCCCACTGCCCCGCACCATCTG GGATGGCGAGCAGAAGACCCACTGCTTTAAAGAACGCACACGATCAC TGCTGCGGGAGTGGTATCTGCAGGACCCTTATCCAAACCCCAGCAAG AAAAGAGAGCTGGCACAGGCCACAGGACTGACTCCAACCCAAGTGG	This study	N/A

(*Continued on next page*)

Continued

REAGENT or RESOURCE	SOURCE	IDENTIFIER
GCAACTGGTTCAAGAATCGGAGACAGCGGGATAGAGCCGCTGCAGC CAAAAATCGACTGCAGCACCAGGCAATTGGCCCCTCCGGGATGCGCT CTCTGGCTGAACCAGGGTGTCCCACTCATGGAAGCGCCGAGTCACCC AGCACCGCTGCAAGTCCTACCACATCAGTCTCTAGTCTGACAGAGAG AGCAGATACTGGCACATCCATCCTGTCCGTGACCTCAAGCGATAGTG AATGCGACGTGTAAACGCGT		
Recombinant DNA		
pLVX-EF1a-tetOn-IRES-G418 (EtO)	Ladewig et al.[32]	Addgene #84776; RRID:Addgene_84776
The Lenti-X Tet-On Advanced System	Clontech	Cat# 632163; N/A
Software and algorithms		
GraphPad Prism	https://Graphpad.com/	RRID:SCR_002798
Zen Imaging Software	Carl Zeiss	RRID:SCR_013672
Fiji	https://ImageJ.net/software/fiji/downloads	N/A
NeuroExplorer	https://www.neuroexplorer.com/	RRID:SCR_001818
Matlab	https://www.mathworks.com/products/matlab.html	RRID:SCR_001622

RESOURCE AVAILABILITY

Lead contact

Further information and requests for resources and reagents should be directed to and will be fulfilled by the lead contact, Satchidananda Panda (panda@salk.edu).

Materials availability

All unique and stable reagents generated in this study of which sufficient quantities exists are available from the lead contact with a complete Materials Transfer Agreement. Direct conversion lentiviral plasmids have been deposited to Addgene #127288 (pLVX- UbC-rtTA-Ngn2:2A:Ascl1).

Data and code availability

No new code was developed or used as part of this manuscript.

The manuscript used published transcriptome data that were downloaded from GEO.

All data reported in this paper will be shared by the lead contact upon request.

EXPERIMENTAL MODEL AND SUBJECT DETAILS

Animals

All experiments including animal experiments were approved and carried out in accordance with the guidelines of the Institutional Animal Care and Use Committee of the Salk Institute. Mice were housed under 12 h light: 12 h dark (LD) cycles. Food and water were available *ad libitum*. C57BL/6J, AVP^{Cre} mice were obtained from the Jackson Laboratory (Strain #:023530). Vip^{Cre} mice was kindly provided by Kuo-Fen Lee's lab.[44] Rorα^{Cre} mouse, which was kindly provided by Dennis O'Leary's lab at the Salk Institute (MGI:5000017), was generated by knocking in an IRES; Cre cassette 3′ downstream of the Rorαlocus.[69] Vip^{Cre}, Avp^{Cre}, and Rorα^{Cre} mice have an IRES; Cre cassette knocked-in downstream of the Vip or Avp or Rorα locus, which permits normal expression of Vip or Avp or Rorα and co-expression of Cre. To generate a mouse in which the nuclei of neuropeptide-expressing are labeled, we used a mouse in which the C terminus of the SUN1 protein, a nuclear membrane protein, was tagged with two tandem copies of superfolder GFP and six copies of the Myc epitope (SUN1-sfGFP-Myc). This transgene was targeted to the ubiquitously expressed Rosa26 locus preceded by a CAG promoter and a loxP-3x polyA-loxP transcriptional roadblock (R26-CAG-LSL-Sun1-sfGFP-myc).[44] The SUN1 fusion protein (SUN1 fused to sfGFP) localizes to the inner nuclear membrane in targeted cell types where promoters driving Cre recombinase are expressed.

METHOD DETAILS

Culture and induction of fibroblasts to neurons

Primary MEFs were isolated from E14.5 mice embryos under a dissection microscope.[18] MEFs were not sex-dependent during isolation. Briefly, after removing the head, vertebral column, dorsal root ganglia, and all internal organs to ensure the removal of all neurogenic potential cells from the embryo, the remaining tissue was dissociated in 0.25% Trypsin (Sigma) for 10 min. The cells were cultured in MEF medium (Dulbecco's Modified Eagle Medium (Invitrogen) containing 10% Fetal Bovine Serum (FBS) (Hyclone), beta-mercaptoethanol (Sigma-Aldrich), non-essential amino acids, sodium pyruvate, and penicillin/streptomycin (all from Invitrogen). Human fibroblast cell lines were obtained from the Coriell Institute, ATCCGM22159 and University Hospital in Erlangen, Germany.[35]

For direct conversion of fibroblasts to neurons, lentiviral particles for pLVX-EtO and ASCL1/NGN2 (AN) (kindly provided by Dr. Mertens, Laboratory of Genetics, Salk Institute for biological studies) and the iN-SCNTF TFs were incubated with the fibroblasts for 20–24 h. Forty-eight hours after transduction, the neuron (iN)- and iN-SCNTF-competent fibroblasts were further passaged in drug selection media with G418 (200 μg/mL; Gibco, Thermo Fisher Scientific) and puromycin (1 μg/mL; Sigma-Aldrich) in tetracycline-free FBS-containing medium.

To generate iNs, cells were cultured for 2 days in tetracycline-free FBS-containing medium with the addition of doxycycline (1 μg/mL, Sigma-Aldrich) before changing to optimized induced neuronal conversion medium, containing a 50:50 base of DMEM:F12/Neurobasal containing the following supplements: N2 supplement, B27 supplement (both 1 ×; Gibco, Thermo Fisher Scientific), doxycycline (2 μg/mL, Sigma-Aldrich), Laminin (1 μg/mL, Life Technologies, Carlsbad, CA, USA), dibutyryl cyclic-AMP (500 μg/mL, Sigma-Aldrich), human recombinant Noggin (150 ng/mL; Peprotech), LDN-193189 (0.5 μM; Cayman Chemical Co, Ann Arbor, MI, USA), A83-1 (0.5 μM; Stemgent, Lexington, MA, USA), CHIR99021 (3 μM, LC Laboratories, Woburn, MA, USA), Forskolin (5 μM, LC Laboratories) and SB-431542 (10 μM; Cayman Chemical Co).[32] The medium was changed every third day.

For further maturation, iNs were switched to neural maturation medium (NMM), containing a 50:50 base of DMEM:F12/Neurobasal containing glial cell–derived neurotrophic factor, brain-derived neurotrophic factor (both 20 ng/mL, R&D Systems, Minneapolis, MN, USA), dibutyryl cyclic-AMP (500 μg/mL, Sigma-Aldrich), doxycycline (2 μg/mL, Sigma-Aldrich) and laminin (1 μg/mL, Life Technologies). For functional analysis of the neurons, iNs were replated on a feeder layer of mouse astrocytes and cultured in NMM for an additional 2–3 weeks.[32]

Vector design and generation of lentiviral particles

The Lenti-X Tet-On Advanced System (Clontech, Mountain View, CA, USA) was modified by replacing the CMV promoter of the pLVX-tetOn Advanced vector with the EF1α promoter, resulting in the pLVX-EtO vector.[32] Coding sequences for the neuronal conversion TFs were synthesized and cloned into the pLVX-Tight-Puro construct (Clontech). The pro-neuronal factors ASCL1 AN were linked by a 2A peptide sequence or target TF sequences based on human ORF before insertion into the pLVX-Tight-Puro vector. The lentiviral vector plasmid, the packaging plasmid, and the envelop plasmid were co-transfected into HEK293FT cells using polyethyleneamine. Resulting viral particles were enriched by ultracentrifugation. They were then frozen for future use.[32]

Immunofluorescence analysis

For immune-histology analysis, cells were fixed in 4% PFA for 20 min at room temperature. The cultured cell sample fixation time was between 11:00 and 15:00 for immunofluorescence analysis. Cells were permeabilized with 0.1% Triton X-100 (Sigma-Aldrich) in PBS for 20 min. Blocking was performed with 10% FCS (Invitrogen) in PBS with 0.1% Triton X-100 for 1 h. Cells were incubated with primary antibodies diluted in blocking solution at room temperature for 2–3 h or overnight, washed twice in PBS, and reacted with secondary antibodies diluted in blocking solution for 45 min, counterstained with DAPI, and mounted with Vectashield mounting solution (Vector Laboratories). Primary antibodies were listed at the Table S2 were applied overnight at 4°C. Secondary antibodies were incubated for 2 h at room temperature. Confocal images were taken on standard fluorescence microscopes or Zeiss LSM710/780 confocal microscopes. All data for one experiment were acquired from cells cultured and processed in parallel on the same microscope with the exact same setting used.

Time-lapse calcium imaging

Six-week-old iNs maintained on primary rat astrocytes were loaded with the calcium-sensitive dye Fluo-4 using the Fluo-4 calcium imaging kit (Life Technologies). Briefly, the iNs were incubated with Fluo-4 (1 μM in Kreb HEPES buffer solution; KHB solution) for 75 min at 37°C. For the preparation of pSCN, cylindrical punches of a unilateral SCN from 2- to 4-day-old pups were collected from 400 μm coronal sections using a 20 gauge needle. Cells were dissociated using papain and cultured,[42] with the medium contained 5% FBS. Cells were maintained in culture for 2 weeks before analysis. Cultured neurons were washed with a KHB solution 4 times and settled for 20 min in an incubator before imaging. Calcium imaging was performed using the Zeiss LSM 880 Rear Port Laser Scanning Confocal and Airyscan FAST Microscope (Carl Zeiss, Germany). Images were obtained using a standard Alexa Fluor 488 filter and were taken every 131 ms, using the 20× objective for a total time of 150 s. Neurons were stained after the analysis to confirm neuronal marker expression. Neurons were outlined as regions of interest and analyzed using IMARIS software (total number of neurons traced: iN = 18; iN-SCNTF = 20; from two separate individuals). For each region of interest, changes in fluorescence intensity over time (Delta F) were plotted. Values were normalized to the minimum fluorescence (F min) for each.

Multi-electrode array recording

Six-week-old iNs or pSCN were maintained on a multi-electrode array (Multichannel Systems, Reutlingen, Germany) in an incubator at 37°C with 5% CO_2. The electrophysiological activity of the neurons was recorded for 3 days via 256 electrodes that were 30 μm in diameter, spaced every 100 μm apart, and arranged in a 16 × 16 square grid (Multi channels systems). Signals were obtained from all 256 channels @ 10 kHz. Negative thresholds for spike detection were set at 5 times the standard deviation of the noise on each channel. Spike cutouts, consisting of 1 msec preceding and 2 msec after a supra-threshold event, along with a timestamp of the trigger, were written to the hard disk. For each electrode, these spike cutouts were sorted into trains of a single cell after recording using Offline Sorter (Plexon, Denton, TX). Data analysis and display were performed using Neuroexplorer (Plexon) and custom software written in MATLAB (Mathworks, Natick, MA).

QUANTIFICATION AND STATISTICAL ANALYSIS

Quantification for βIII-tub and the calculation for the conversion yield of MEF or human fibroblasts, and quantification for co-staining immunofluorescein analysis are based on at least three independent experiments. Quantitative data statistics were calculated using GraphPad Prism software with the method indicated for each figure or STAR methods section; for control or iN versus iN-SCNTF comparisons, unpaired t tests and ANOVAs were used. Significance evaluations are marked as *$p < 0.05$; **$p < 0.01$ in the figures. Statistical analysis of rhythmic firing: We used meta2d, a function of the R package MetaCycle, to evaluate periodicity in the time series.[70] Briefly, meta2D incorporates ARSER,[71] JTK_CYCLE,[72] and Lomb-Scargle[73] algorithms and it implements N-version programming concepts to integrate their results including p values, period, and amplitude. Neurons were considered to fire rhythmically when the integrated p value was <0.05 and a period between 18 and 30 h.